https://doi.org/10.5194/egusphere-2026-1502
Preprint. Discussion started: 13 April 2026

A dynamic socio-hydrology model for the assessment of time-variant feedbacks between irrigators' adaptive responses and basin hydrology

Osama Hassan[1,2], Francesco Sapino[1], Héctor González-López[1,2], C. Dionisio Pérez-Blanco[1,3]

[1]Economic and Institutional Analysis Group, IMDEA Water Institute, Madrid, 28805, Spain
[2]Department of Economics and Business Management, University of Alcalá, Madrid, 28805, Spain
[3]Euro-Mediterranean Center on Climate Change, Via della Libertà, 12, 30121 Venezia VE, Italy

Correspondence to: Osama Hassan (Osama.hassan@edu.uah.es)

Abstract. This study introduces a Dynamic Feedback (DF) socio-hydrology model that couples the widely used SWAT hydrological model with a microeconomic model of irrigators' behavior (Positive Multi-Attribute Utility Programming Model). Unlike conventional static or exogenous scenario-based socio-hydrology couplings, the DF setup allows irrigators' adaptive responses and basin hydrology to interact dynamically through time-variant two-way endogenous exchanges. The model is illustrated with an application to the Tormes catchment in Spain, where we assess the impacts of a Drought Management Plan (DMP) that introduces water caps to ensure environmental flows under alternative climate change scenarios (SSP126 and SSP585), using both a DF and no-feedback setup. Aggregate results indicate relatively small differences between the DF and no-feedback setup in annual hydrological indicators across the Tormes catchment (<0.5%). Critically, differences become significant at sub-basin and seasonal scales, where adaptive irrigators' responses to DMP caps during dry years in the DF setup increase summer inflows by up to 9.3% under SSP585 as compared to the no-feedback setup, signaling higher effectiveness of DMP interventions.

https://doi.org/10.5194/egusphere-2026-1502
Preprint. Discussion started: 13 April 2026

1 Introduction

Socio-hydrology emphasizes two-way feedbacks modeling to understand, and where possible forecast, emergent phenomena in which coupled human-water socio-ecological systems (SES) exhibit properties and behaviors that do not exist in isolated hydrological or economic models alone—but rather emerge through interactions within the broader interconnected system (Di Baldassarre et al., 2019; Vanelli et al., 2022). Accordingly, a critical aspect in the representation of human-water feedbacks and emergent phenomena in socio-hydrology is sub-model coupling (Expósito et al., 2020; Han et al., 2025). The two overarching approaches in sub-model coupling are integrated coupling, which merges the relevant hydrological and socioeconomic processes into a single modeling framework (Harms et al., 2023; Harou et al., 2010; Souza da Silva and de Moraes, 2018); and modular coupling, where independent modules are populated with full-fledged socioeconomic and hydrological models and subsequently interconnected through information exchange rules known as protocols (Essenfelder et al., 2018; Jeuland, 2010; Kahil et al., 2015) .

Integrated coupling approaches adopt simple conceptual models that endogenize feedbacks to study the dynamic co-evolution of water–human systems. Full model integration comes at the expense of detail in the economic sub-model, which represents human behavior with stylized differential equations (such as a piecewise demand function) that are subsequently integrated into the hydrological sub-model (Soriano et al., 2025). This has led to the criticism of the ability of integrated coupling approaches to capture co-evolution dynamics, particularly those driven by the adaptive behavior from human agents (Franzke et al., 2022; Konar et al., 2019). In this context, modular studies are growing as an alternative that enables higher behavioral resolution and heterogeneity by introducing full-fledged representations of human agents.

Key limitations to modular models include their higher computational cost and the temporal and spatial mismatches between modules, which can lead to unstable or delayed feedback loops and data loss (Blair and Buytaert, 2015; Laniak et al., 2013; Voinov and Shugart, 2013). While recent advances in computational power and techniques have made it increasingly feasible to run complex modular models (Fischer et al., 2021), and recent research has explored novel coupling protocols to address spatial mismatches (Di Baldassarre et al., 2013; Essenfelder et al., 2018; Roobavannan et al., 2020), temporal mismatches remain a fundamental barrier for modular coupling, making dynamic feedbacks “difficult to model”(Fischer et al., 2021). Accordingly, exchanges between modules typically happen before the model simulation starts or after the model simulation has been completed (i.e., one model is run from year 1 to T, and the information thus generated is incorporated into another model that is subsequently run from year 1 to T). This can be done by having a single information exchange between modules or leveraging scenario-based simulations with predefined adaptation logic, where the socioeconomic model is pre-run under a number of (policy, economic, other) scenarios and the simulation results thus obtained are used as time-variant forcings to the hydrological model in a subsequent run (e.g., as exogenous land use forcings over time) (Choi and Deal, 2008; Gandolfi et al., 2014; Getachew et al., 2021; Nie et al., 2011). Note that in these modular couplings, adaptation is triggered exogenously through prior scenario assumptions (e.g., fixed policy or economic conditions), rather than endogenously responding to emergent water stress, which risks losing relevant co-evolution information—particularly under non-stationary conditions such

https://doi.org/10.5194/egusphere-2026-1502
Preprint. Discussion started: 13 April 2026

as climate change. In reality, since system conditions in year *t* depend on the status of the system in year *t-1*, when a dynamic hydrological (socioeconomic) model starts running a simulation encompassing multiple periods, communication with the socioeconomic (hydrological) model typically should be taking place in between these periods (and not at the beginning or the end), as happens in integrated coupled models.

This paper aims to bridge this gap by building a protocol that enables inter-annual dynamic feedback (DF) coupling between full-fledged hydrological and socioeconomic models. Since the intended protocol needs to be adapted to the specific model, and in order to make our approach as scalable and replicable as possible, we have chosen two widely used models within the community for the coupling: the Soil and Water Assessment Tool (SWAT) (Arnold et al., 1998), which can represent complex hydrological processes at different scales and contexts, especially in agriculture and watershed management (Samimi et al., 2020); and microeconomic Mathematical Programming Models (MPM), the most widely used socioeconomic approach to model farmers' behavior (Soriano et al., 2025). SWAT is a paradigmatic example of the coupling limitations in modular socio-hydrology frameworks mentioned above, with existing SWAT–economic couplings (Bouzidi and Pérez-Blanco, 2025; Essenfelder et al., 2018) depending on fixed scenario-based simulations where the socioeconomic model is pre-run and the simulation results are used as forcings to the hydrological model subsequently. The DF coupling protocol is implemented through a customized SWAT model in Fortran language referred to as SWAT-DF that is openly available at https://github.com/oshs/SWAT-DF. Our approach is illustrated with an application to the Tormes catchment in southwest Spain, a semi-arid agricultural basin increasingly vulnerable to climate extremes, where we assess the performance of DF vs. no-feedback setup (noDF) under climate change scenarios.

2 Case Study

The Tormes catchment covers approximately 7116 km2 and has two reservoirs, Santa Teresa and Almendra. Hydropower production is the primary economic use in the Almendra, whereas the Santa Teresa reservoir is used to regulate and manage water flows and supplies to irrigation (See Fig. 1).

https://doi.org/10.5194/egusphere-2026-1502
Preprint. Discussion started: 13 April 2026

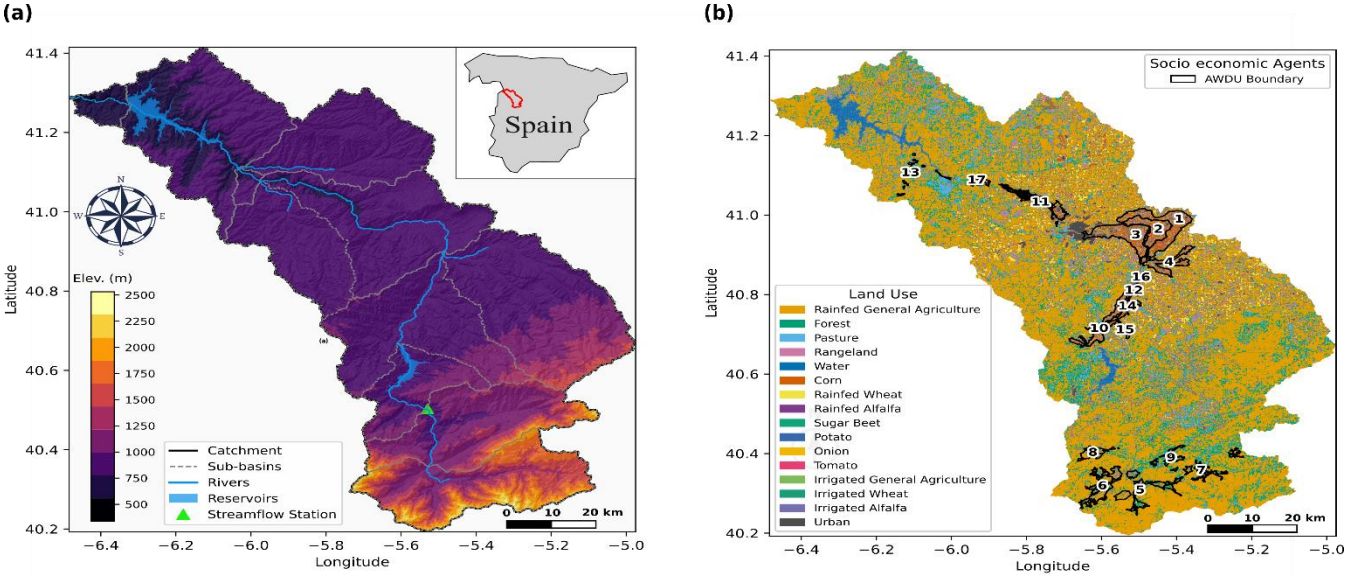

Figure 1: (a) Study area characteristics, and (b) spatial distribution of socioeconomic agents with land use map.

The Tormes is an agricultural catchment encompassing a total irrigated area of 17,596 ha, divided into 17 Agricultural Water Demand Units (AWDUs)i.e. socioeconomic agents, 5 located upstream of the Santa Teresa reservoir and 12 downstream. In the Spanish water management framework, an AWDU is a standardized spatial and administrative unit used to quantify and allocate agricultural water based on local soil properties, crop types, and irrigation technologies.

For the purposes of the socio-hydrological coupling in this study, each spatial AWDU is represented in the microeconomic model (PMAUP) by a single, aggregate socio-economic agent. This representative agent acts as a proxy for the collective decision-making of the farmers within that AWDU, optimizing the crop portfolio and water use in response to the dynamic water availability constraints.

The Duero River Basin Authority or Confederación Hidrográfica del Duero (DRBA, 2018) indicates that the annual available water volume in the Tormes catchment is 1,300 MCM, based on the average from 1980/81 to 2005/06. The average yearly total water demand in the catchment is 635 MCM, with 93% of this demand situated upstream of Santa Teresa reservoir. Of the total demand, 45% is allocated for irrigation, of which 251.39 MCM annually is used upstream Santa Teresa reservoir and 34.36 MCM downstream. The remaining 55% of the demand is allocated to urban, industrial, fish farms, and recreational uses, most of which are non-consumptive.

Climate change is anticipated to intensify rainfall volatility and gradually reduce the availability of water resources, aggravating water scarcity and droughts (CEDEX, 2023). The catchment has already experienced drought episodes since 1944, varying from light to moderate severity, and a drought management plan was adopted in 2007 (updated in 2018), aiming to minimize socioeconomic and environmental impacts (DRBA, 2018). This plan included the implementation of drought indicators to monitor the situation monthly, with four possible drought status existing: Normality (no drought), Pre-Alert, Alert, and Emergency, each of which is conditional on predefined water storage volume thresholds in Santa Teresa reservoir.

https://doi.org/10.5194/egusphere-2026-1502
Preprint. Discussion started: 13 April 2026

A historical analysis spanning from 1980 to 2017 identified the thresholds for determining the drought status (Fig. 2), each of which may trigger restrictions for agricultural water use (Table 1).

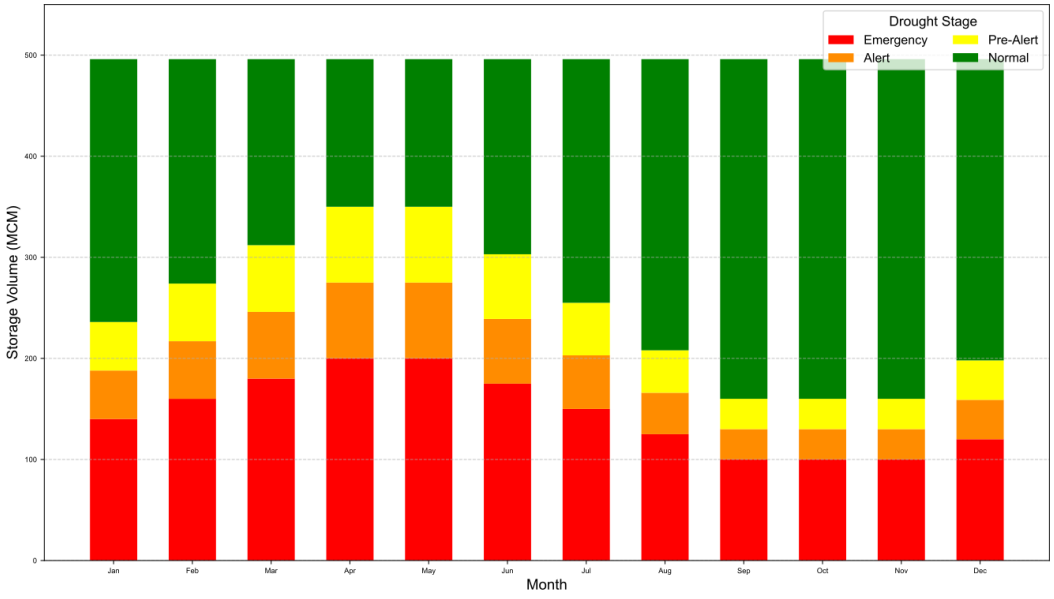

Figure 2: Monthly storage volume thresholds for Pre-Alert, Alert, and Emergency drought for Tormes catchment.

Table 1: Water Reduction (WR) for agriculture under drought, Tormes catchment.

Status situations	Lack of shortage	Moderate shortage	Severe shortage	Serious shortage
Scarcity scenarios	Normal	Pre-Alert	Alert	Emergency
Measures	General planning and monitoring (0% WR)	25% water reduction (25% WR)	50% water reduction (50% WR)	100% water reduction (100% WR)

3 Methods and data

The methodology we propose employs two-way DF coupling protocol between the SWAT hydrological model and a microeconomic MPM. Specifically, we utilize the Positive Multi-Attribute Utility Programming model (PMAUP) as MPM (other MPM such as Positive Mathematical Programming or Linear Programming (LP) can also use our DF coupling protocol with SWAT without the need for further refinements of the approach). The DF protocol is designed to capture the reciprocal interactions between water availability, policy-driven water allocation constraints, and adaptive land use (and related water

https://doi.org/10.5194/egusphere-2026-1502
Preprint. Discussion started: 13 April 2026

use) decisions under changing climatic conditions. The following subsections present the two-way DF coupling protocol (Sect. 3.1), the SWAT hydrological model (Sect. 3.2), the PMAUP microeconomic model (Sect. 3.3), and the data used for the model calibration and climate change scenarios (Sect. 3.4).

3.1 Two-way dynamic feedback (DF) protocol

The essence of our DF protocol is based on the interplay between land use decisions (crop portfolio) as simulated by the PMAUP model, and the water availability attributed to key water system variables under climate change scenarios, which is simulated by the SWAT model. Unlike conventional static or exogenous scenario-based socio-hydrology modular couplings, our model resolves these interactions endogenously at an annual timestep over multiple years (interannual), to reflect the temporal scale at which farming decisions and water allocation policies are typically implemented and the coevolution of the human and water systems.

Spatially, the framework builds on the Hydrologic Economic Response Unit (HERU) concept (Essenfelder et al., 2018). Traditional SWAT Hydrologic Response Units (HRUs), defined by land use, soil, and topography, are combined with spatially defined socio-economic agents (AWDU) to form integrated modeling units. Readers are referred to Essenfelder et al. (2018) for a detailed description of the HERU methodology.

The DF protocol was implemented through a customized SWAT referred to as **SWAT-DF** that is openly available here (https://github.com/oshs/SWAT-DF). The DF implementation modifies the SWAT Fortran source code by introducing a dedicated module to read PMAUP outputs at each interannual coupling step. PMAUP provides updated crop portfolio changes, which are translated into HRU-level fractional areas (hru_fr) for each water restriction scenario (WR); these files are stored alongside the SWAT model and used by the modified **SWAT-DF** code during execution to dynamically update land and water use. The study framework is conceptually depicted in Fig. 3 and the feedback simulation in Fig. 4.

https://doi.org/10.5194/egusphere-2026-1502
Preprint. Discussion started: 13 April 2026

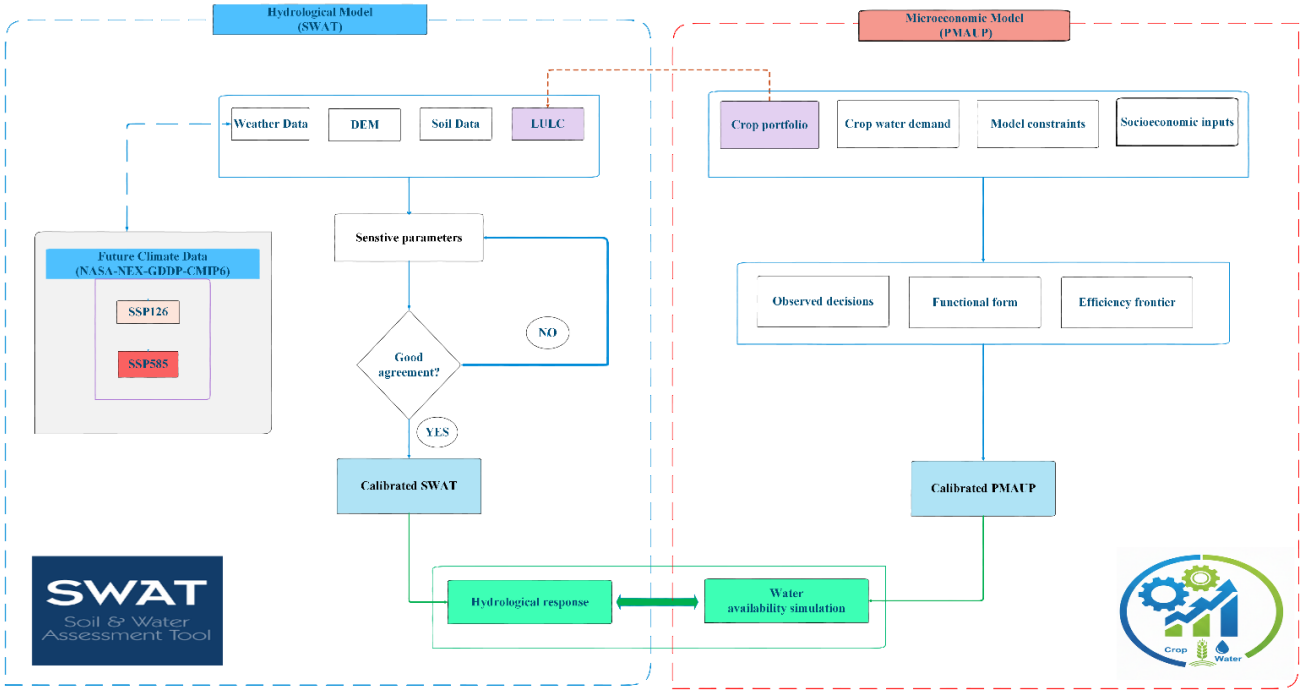

Figure 3: Conceptual framework of the dynamic feedback (DF) coupling between the hydrological model (SWAT) and the microeconomic model (PMAUP).

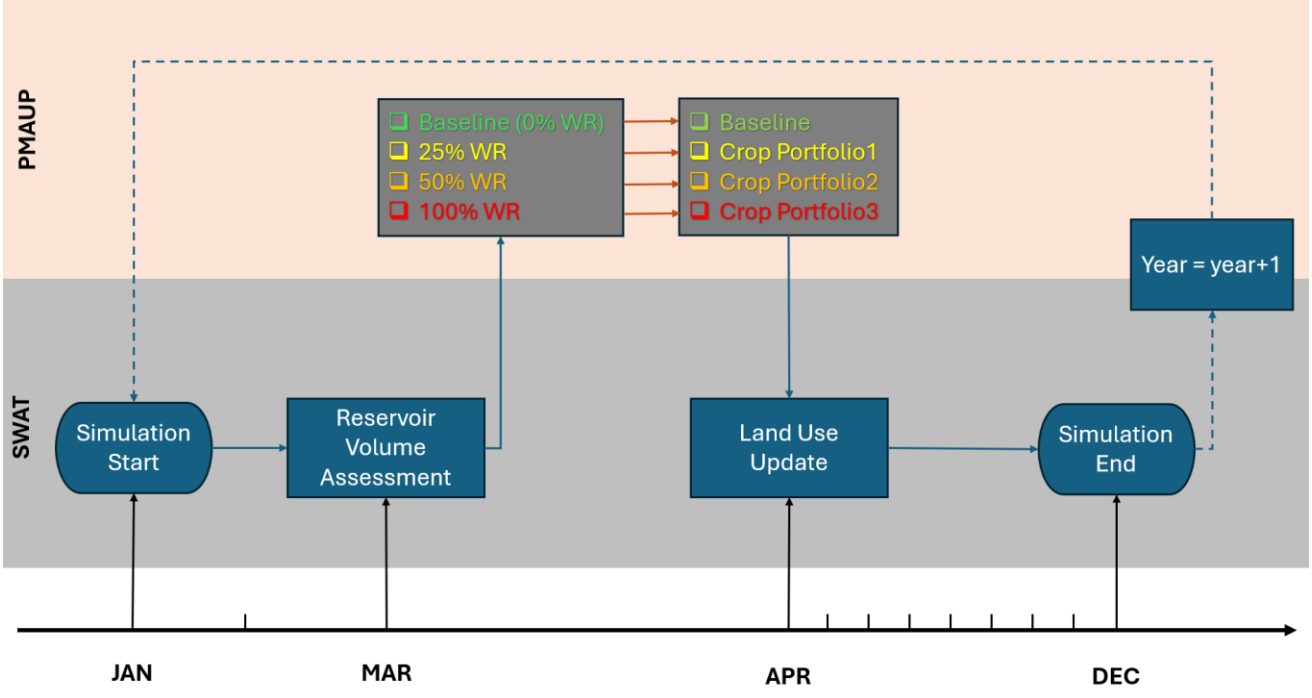

135 **Figure 4: Dynamic feedback (DF) implementation feedback between SWAT and PMAUP.**

https://doi.org/10.5194/egusphere-2026-1502
Preprint. Discussion started: 13 April 2026

Our two-way DF protocol begins with the SWAT (Sect. 3.2) assessing the water availability for irrigation resulting from hydrological simulations and water management in the reservoir under the climate change scenarios in year (t). To this end, the model produces monthly streamflow and reservoir volume which represents water availability. Next, the simulated storage volume in March ($V_m(t)$, beginning of the irrigation campaign) is compared against the drought thresholds for the Tormes catchment established in the drought management plan (see Fig. 2), and one of the four water reduction measures in Table 1 is activated. These restrictions define the water allotted to agriculture in the ongoing season.

Next, the PMAUP model (Sect. 3.3) uses this information to simulate adaptive farmer responses, including changes in land and water allocation across different crop types per AWDU for year (t). The resulting crop portfolio is translated into updated land-use shares at HRU and applied to the SWAT model to define the land-use configuration for the remainder of the year (t). The previous steps are repeated annually over the simulation period allowing land-use patterns, water availability, and policy responses to co-evolve over time, creating an iterative two-way DF loop that *dynamically* captures how socioeconomic responses to water availability influence hydrological conditions, and vice versa, enhancing our understanding of the complex interdependencies within SES and informing adaptive policy and management strategies in the context of climate change.

3.2 Hydrological model (SWAT)

SWAT model is a widely utilized open-source tool for modeling various hydrological processes such as runoff, sediment yield, nutrient transport, pesticide loss, and the impact of climate change (Gassman et al., 2014; Reshma and Arunkumar, 2023; Yen et al., 2019). SWAT model functions as a continuous-time, process-based, semi-distributed hydrological framework. The primary input data for the model are Digital Elevation Model (DEM), land use and land cover (LULC) data, soil data, and climate variables. Within the SWAT framework, basins are separated into several sub-basins, which are then broken down into HRUs that represent different combinations of land use, soil, and slope attributes. Hydrological variables are simulated at the HRU level and then combined at basin scale. Leveraging its capability to simulate both hydrological processes and land use management actions, SWAT serves as a relevant tool for assessing the impact of climate change on water availability (Haider et al., 2023; Zhang and He, 2023).

The R-SWAT Tool provides an R-based interface for automated sensitivity analysis, calibration, and validation of SWAT models using observed hydrological data. In this study, it was employed for performing model sensitivity, calibration and validation analysis (Nguyen et al., 2022). Parameter sensitivity analysis was developed using MORRIS One-At-a-Time Elementary Effects (OAT-EE) screening method (Morris, 1991). Sixteen parameters were selected to perform the sensitivity from 1998 to 2014 with three years of warm-up (1995-1997). The parameters ranges were obtained from the literature review. MORRIS method was designed with 20 Trajectories and 5 levels for each parameter space which results in a total of 300 simulations of sensitivity analysis. Two metrics were used to assess the sensitivity analysis of a parameter, absolute mean of the Elementary Effect (EE_absμ) and the standard deviation of the Elementary Effect (EE_δ). Higher EE_absμ indicates higher sensitivity while higher (EE_δ) indicates higher sensitivity order and interaction with other parameters.

https://doi.org/10.5194/egusphere-2026-1502
Preprint. Discussion started: 13 April 2026

Calibration performance was measured against the observed streamflow on a monthly basis, with the Nash-Sutcliffe Efficiency (NSE) set as the objective function. The calibration period spanned from 1998 to 2009 with 1000 simulations using Latin Hypercube Sampling (LHS) sampling method while the validation was conducted from 2010 to 2014. SWAT model performance was assessed using three metrics: NSE, Root Mean Standard Deviation Ratio (RSR), and Percent Bias (PBIAS).

3.3 Microeconomic model (PMAUP)

Microeconomic MPM are analytical tools for examining and evaluating how irrigators allocate land and water resources within constraints (Gutierrez-Martin and Gomez, 2011). In positive MPM, the agents or irrigators (grouped in AWDUs in our case) decide on the land share allocated to each crop X_i ($i = 1, \dots n$), or crop portfolio (X), to maximize the utility (U(X)) derived from one (single-attribute MPM, including profit) or multiple (multi-attribute MPM, as is the case of PMAUP, including profit, risk aversion, and management complexity avoidance, among others) attributes (Z(X)), within a domain (F(X)) conformed by physical and socioeconomic constraints including water availability (W(WR), which in our coupled model is a function of the water reduction determined through SWAT simulations and the water restrictions in Table 1):

$$Max\ U(X)_x = U(Z_1(X); Z_2(X); Z_3(X); Z_4(X) \dots Z_m(X)) \quad (1)$$

$$s.t: 0 \le X_i \le 1 \quad (2)$$

$$\sum_{i=1}^{n} X_i = 1 \quad (3)$$

$$X \in F(X) \quad (4)$$

$$Z = Z(X) \in R^m \quad (5)$$

$$\sum_{i=1}^{n} W_c \,.\, X_c \le W(WR) \quad (6)$$

Section S2 in the online Supplementary Materials presents the relevant attributes used in the PMAUP utility function, which include Profit (Z1), Risk avoidance (Z2), and Management complexity (Z3); while Sect. S1 presents the constraints that conform the domain, including the water availability constraint W(WR).

Positive MPM calibrate an objective function to observed decisions, aiming at minimizing the difference between simulated and observed decisions. The fundamental differences between MPM emerge from the calibration method adopted, with a marked division between multi-attribute (such as PMAUP) and single-attribute models. The calibration process of the PMAUP model is presented in detail in Sect. S3 of the Supplementary Materials. A comparative analysis of the different MPM, including PMAUP and other widely used models such as Positive Mathematical Programming (PMP) or Linear Programming, is provided by (Sapino et al., 2020) .

https://doi.org/10.5194/egusphere-2026-1502
Preprint. Discussion started: 13 April 2026

3.4 Data

3.4.1 Climate change scenarios

The impact of climate change was evaluated using ten different CMIP6 Global Climate Models (GCMs): ACCESS-CM2, CanESM5, CMCC-ESM2, CNRM-CM-1, EC-Earth3, GFDL-ESM4, IPSL-CM6A-LR, MIROC6, MPI-ESM1-2-HR, and MRI-ESM2-0. CMIP6 data from these models were acquired from NASA Earth Exchange Global Daily Downscaled Projections (Thrasher et al., 2022) . The data is bias corrected and downscaled using the Bias-Correction Spatial Disaggregation (BCSD) method, achieving a finer spatial resolution of 0.25° * 0.25°. The dataset included daily precipitation, maximum and minimum temperatures, covering the future projections for two Shared Socioeconomic Pathways (SSPs): SSP126, and SSP585 from 2020-2050. SSP126 and SSP585 represent contrasting low-emission and high-emission scenarios. A Multi-Model Ensemble Average (MMEA) approach was adopted, aggregating the outputs from all ten models (2020-2050) for precipitation and temperature weather variables, for each SSP (i.e., one ensemble average for each SSP and weather variable was produced). The ensembled data for precipitation and temperature for each SSP were used as weather data inputs in the SWAT model to examine the impacts of climate change (both SSP126 and SSP585) on hydrological outputs.

3.4.2 Hydrological data

The SWAT model requires several key inputs for simulating streamflow including DEM, land use and land cover, soil data, meteorological data, and hydrological data. SWAT model inputs are shown in Table 2.

https://doi.org/10.5194/egusphere-2026-1502
Preprint. Discussion started: 13 April 2026

Table 2: SWAT model inputs.

Data Type	Data Provider	Resolution	Description	Ref Year/Period
DEM	(IGN, 2020)	25m	DEM	2014
Land use/cover	(IGN, 2020)	Scale 1:100.000	Sistema de Información de Ocupación del Suelo de España-Corine Land Cover (SIOSE-CLC)	2018
Soil data	(ESD, 2004)	Scale 1:1,000,000	Soil Geographical DataBase Eurasia (SGDBE) v2.0	2017
Socioeconomic agents	(DRBA, 2018)	-	AWDUs delineation and crop portfolios (shapefile)	2016
Meteorological data	(Senent-Aparicio et al., 2021)	5km	Daily precipitation, maximum, and minimum temperature	1995 - 2014
	(Fuka et al., 2014)	38km	Daily wind speed, relative humidity, and solar radiation	1995 - 2014
Hydrological data	(CEDEX, 2023)	-	Streamflow	1998 - 2014
			Reservoirs operation	1995 - 2015

3.4.3 Socioeconomic data

The PMAUP model relies on various physical and socioeconomic inputs for model calibration and simulation. Data inputs are summarized in Table 3. Since data inputs from the microeconomic model are located in disparate sources that often require substantial elaboration (e.g., aggregating data into the relevant spatial scale (AWDUs)), the complete database is openly available via Zenodo (https://doi.org/10.5281/zenodo.18543335).

https://doi.org/10.5194/egusphere-2026-1502
Preprint. Discussion started: 13 April 2026

Table 3: PMAUP model inputs.

ID	Data Provider	Description	Ref Year/Period
Water withdrawal and allotment	(DRBA, 2018)	Water withdrawals and allotment for each AWDU	2015
Water requirements and irrigation technology	(DRBA, 2018)	Crop water requirements, conveyance, distribution, and irrigation /efficiency for each AWDU	2015
Crop portfolio	(DRBA, 2018)	Crop information (ha/crop)	2015
Crop yields, and prices	(MAGRAMA, 2015a)	Crop yields, and prices	2004 - 2015
Labor, and crop costs	(MAGRAMA, 2015b)	Working days, variable costs, and other costs	2004 - 2015
Other revenues	(MAGRAMA, 2015b)	Subsidies, insurance payments, and other revenues	2004 - 2015

4 Results and discussion

This section presents the performance of the SWAT model during the calibration and validation period as well as the calibration of the PMAUP model and the two-way Dynamic feedback simulations.

4.1 Calibration and validation results

4.1.1 SWAT model

The results of sensitivity analysis showed that 11 out of the 16 parameters were sensitive parameters with high mean of EE and high standard deviation of EE. SCS curve number (CN_2.mgt) parameter was found to be the most sensitive parameter with (EE_absμ) of 0.33 and (EE_δ) of 0.29, followed by average slope of the HRU (HRU_SLP.hru) with (EE_absμ) of 0.3 and (EE_δ) of 0.44. On the other hand, groundwater revap coefficient (GW_REVAP.gw) parameter was found not sensitive. The 11 parameters were used for the calibration and validation period. Detailed sensitivity results and optimized calibration parameter values are provided in Appendix B.

https://doi.org/10.5194/egusphere-2026-1502
Preprint. Discussion started: 13 April 2026

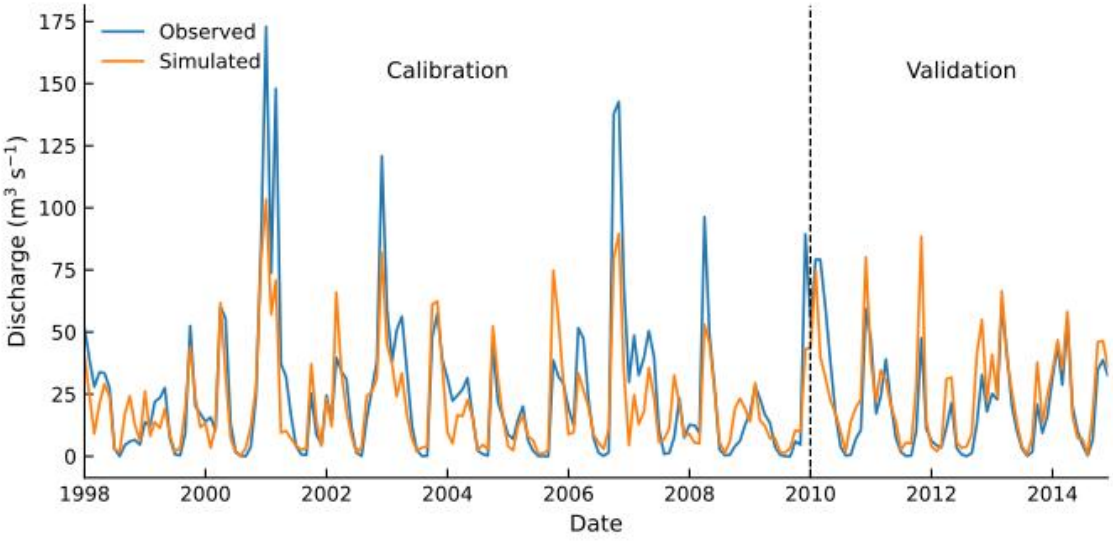

Figure 5: SWAT model performance during calibration (1998-2009) and validation (2010-2014) period.

Figure 5 depicts the model performance during the calibration and validation period on Monthly timestep. As we can see, the model was able to capture the variability in streamflow and shows a good match between the simulated and observed streamflow. The model's performance in predicting peak flows is generally satisfactory with the model performing better in simulating low flows compared to peak flows.

Table 4 summarizes the performance metrics of the model during calibration and validation periods. According to Moriasi et al. (2007), the model demonstrates good performance with NSE of 0.70, 0.65 for calibration and validation periods, respectively. This is further supported by RSR and PBIAS, R^2 values.

Table 4: Performance metrics for the SWAT model during calibration and validation periods.

Performance Metric	Calibration (1998 - 2009)	Validation (2010 – 2014)
NSE	0.70(Good)	0.65(Good)
PBIAS (%)	-18.80(Satisfactory)	19.54(Satisfactory)
RSR	0.54(Good)	0.60(Good)
R^2	0.76	0.71

4.1.2 PMAUP model

The calibration of the PMAUP model was conducted to parameterize the utility function attributes following the calibration procedure described in the Supplementary Materials Sect. S3. The relevant attributes include Profit ($Z1_{)}$, Risk avoidance (Z2), and Management complexity avoidance (Z3) (see Sect. S4) for a mathematical statement of each attribute), whose corresponding parameters are α_1, α_2, α_3, respectively. These attributes were calibrated for each AWDU individually using 2015 as the calibration year. The performance of the model calibration was evaluated using four metrics: Attribute efficiency frontier

https://doi.org/10.5194/egusphere-2026-1502
Preprint. Discussion started: 13 April 2026

error (e_f) which measures the distance between the observed attributes and the attribute efficiency frontier; crop profile calibration error (e_x) which measures the relative distance between the observed crop pattern and the optimal crop profile; the attribute calibration error (e_τ) which quantifies the distance between the observed attributes and the calibrated ones; and the mean calibration error that averages all three errors (e). Calibration results are shown in Table 5.

Table 5: PMAUP calibration results.

AWDU	α_1	α_2	α_3	e_f (%)	e_x (%)	e_τ (%)	e (%)
1	1.00	0.00	0.00	1.33	1.38	1.46	0.80
2	1.00	0.00	0.00	61.00	4.00	2.32	2.94
3	1.00	0.00	0.00	61.61	2.32	1.31	1.19
4	1.00	0.00	0.00	0.69	2.06	0.96	0.79
5	0.81	0.11	0.07	2.71	4.46	4.15	2.22
6	0.89	0.03	0.07	2.56	4.15	4.64	4.49
7	0.86	0.07	0.07	1.84	2.03	3.42	2.92
8	1.00	0.00	0.00	64.43	4.15	4.51	4.40
9	0.99	0.01	0.00	0.92	0.62	4.10	1.41
10	1.00	0.00	0.00	60.42	11.22	4.90	10.98
11	1.00	0.00	0.00	5.72	9.76	5.74	4.23
12	1.00	0.00	0.00	3.37	4.60	6.12	2.79
13	1.00	0.00	0.00	1.66	2.77	2.84	1.43
14	1.00	0.00	0.00	1.58	0.80	1.61	0.80
15	0.99	0.01	0.00	19.12	10.10	2.62	8.28
16	0.60	0.22	0.17	8.99	3.51	3.68	3.09
17	0.98	0.02	0.00	7.64	1.02	7.71	3.63

Table 5 reveals that the profit parameter (α_1) appeared as the most influential attribute in decision-making for the majority of AWDUs, with α_1 values equal to 1 in several basins (akin to single-attribute MPM). This indicates that there is a significant preference for maximizing the expected profit among agents. The parameter values for risk avoidance (α_2) and management complexity avoidance (α_3) were lower, indicating that they were less significant in explaining decision-making compared to profit. The model performed well with mean average calibration (e) less than 10% for all AWDUs except for AWDU 10 with e of 10.98% (Gómez-Limón et al., 2016).

https://doi.org/10.5194/egusphere-2026-1502
Preprint. Discussion started: 13 April 2026

4.2 Climate change scenarios

Figure 6 illustrates the observed historical (1980-2010) and projected future patterns (2020-2050) of precipitation, maximum and minimum temperature under SSP126 and SSP585, highlighting both annual and seasonal variations in precipitation and temperature. Additional details on the climate data are provided in Appendix A.

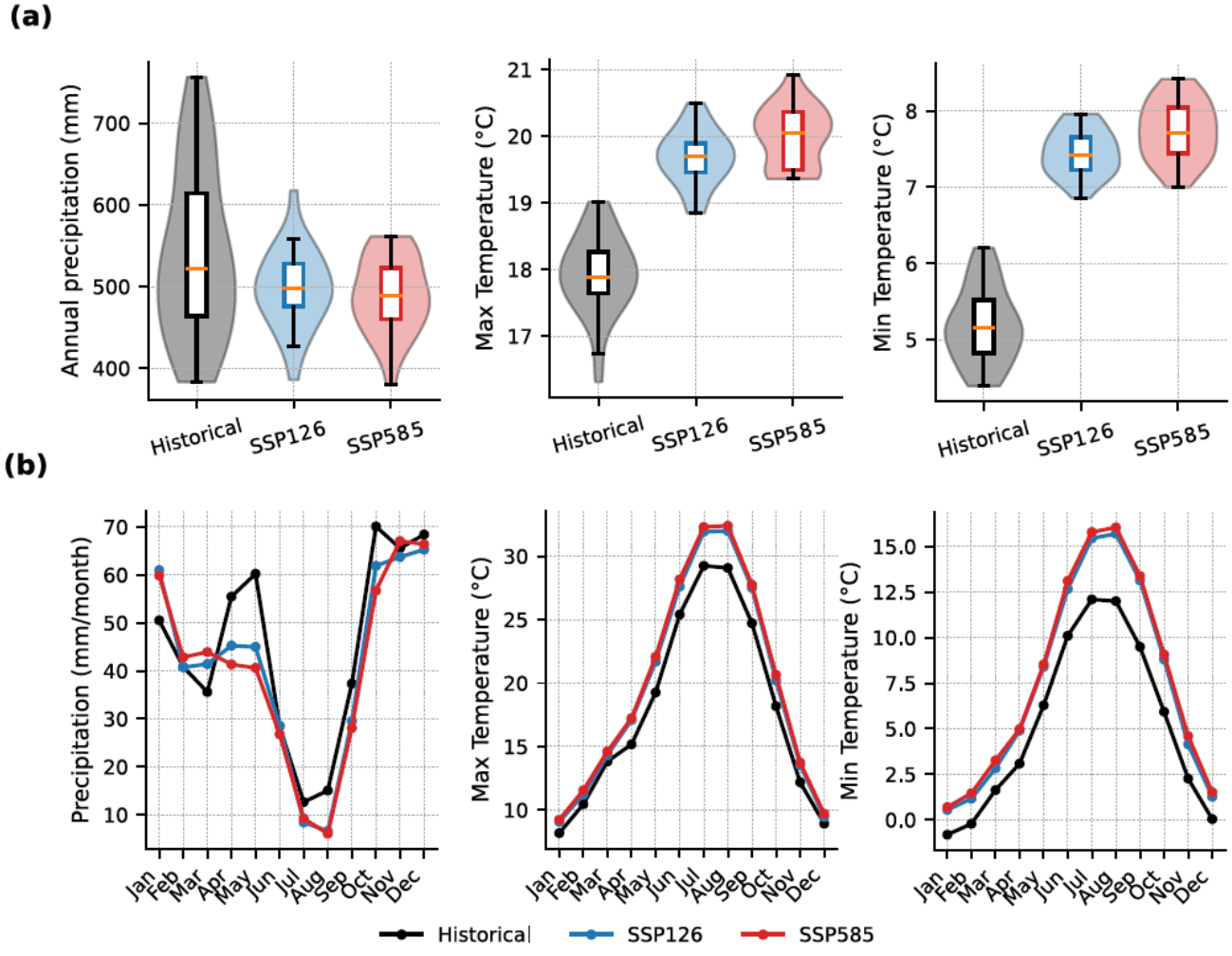

Figure 6: Observed Historical (1980-2010) and future climate change scenarios (2020-2050) under SSP126 and SSP585: (a) annual precipitation, maximum temperature, and minimum temperature; (b) mean monthly precipitation, maximum temperature, and minimum temperature.

Panel (a) shows that the projected precipitation under both SSPs exhibits a modest decline compared to the observed historical baseline. Mean annual precipitation decreases from 540.2 mm during the historical period to 497.4 mm and 488.9 mm under SSP126, SSP585 respectively. Conversely, the projected maximum and minimum temperature increase consistently under

https://doi.org/10.5194/egusphere-2026-1502
Preprint. Discussion started: 13 April 2026

both SSPs with more pronounced warming under SSP585. Mean maximum temperature increases by 1.8°C, 2.1°C under SSP126, SSP585 respectively, while mean annual minimum temperature rises by 2.3°C and 2.6°C.

Panel (b) demonstrates that these shifts exhibit seasonal heterogeneity. projected reductions in precipitation are most severe during the late spring and summer months, aligning with the peak irrigation season, whilst winter precipitation exhibits very minor alterations. Temperature rises occur throughout the seasons but are intensified in summer, exhibiting higher maximum and minimum temperatures. Overall, these trends suggest a future climate marked by warmer temperatures during essential agricultural phases, hence necessitating the integration of dynamic water management and adaptation strategies.

4.3 Simulation results

Leveraging the calibrated SWAT and PMAUP models in Sect. 4.1 we run the SWAT model with the climate change scenarios in Sect. 4.2 to assess the hydrological and socioeconomic impacts of climate change under DF vs. a conventional model (noDF) where SWAT is run dynamically with no yearly interannual interaction with the PMAUP model. To transform hydrological impacts into water allocations to socioeconomic agents, we rely on the drought management plan of the Tormes catchment.

4.3.1 Catchment-scale yearly hydrological results

Figure 7 illustrates the simulation of March reservoir storage at Santa Teresa reservoir from 2020 to 2050 under the SSP126 and SSP585 scenarios, alongside the drought management thresholds that determine the use of water restriction (WR) measures. It demonstrates how the dynamic feedback (DF) approach translates simulated hydrological conditions into yearly constraints into the PMAUP model by triggering WR, which in turn results in land and water use changes that affect next year's SWAT results (including WR). This DF process cannot be simulated with the conventional noDF approach (no yearly interannual interaction) and explains the differences in the simulation results between both approaches.

https://doi.org/10.5194/egusphere-2026-1502
Preprint. Discussion started: 13 April 2026

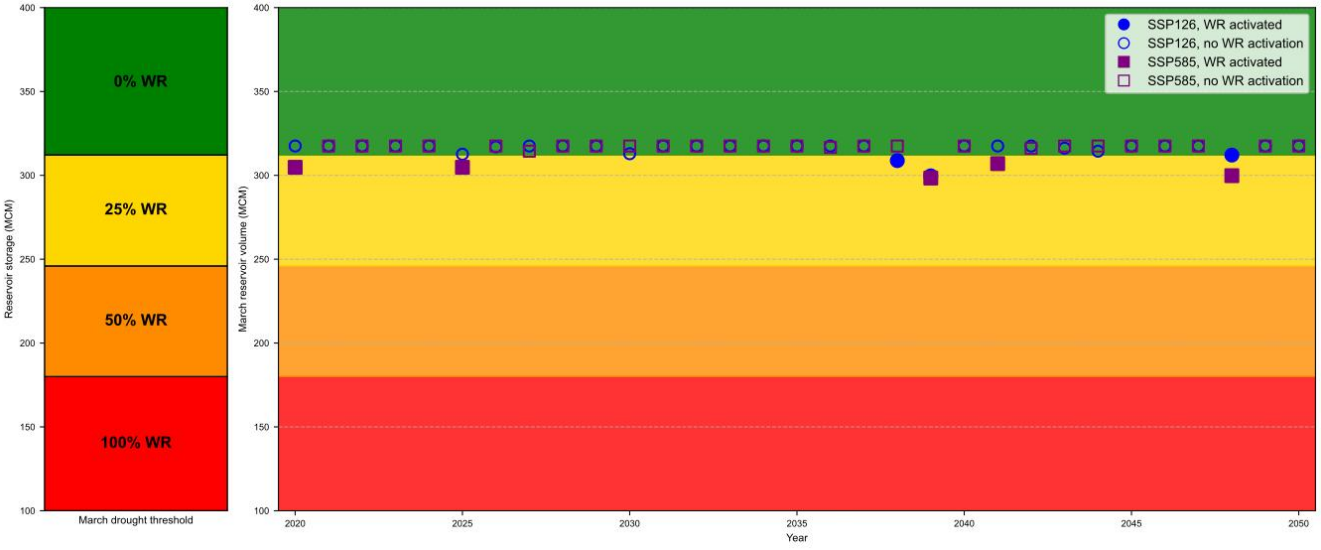

Figure 7: The interactive dynamic coupling over yearly timestep using the drought management plan of March under SSP126 and SSP585. Filled rectangles and circles indicate a water reduction activation (% WR).

Under SSP126 scenario, March reservoir storage remains within the Normal (0% WR) range for most of the simulated period. However, threshold activation occurs in 2038, 2039, and 2048, triggering 25% WR (Pre-Alert status). Storage values demonstrate small inter-annual fluctuation and are consistently outside the Alert and Emergency conditions. This trend indicates the relatively modest hydroclimatic stress linked to the low-emission pathway, leading to consistent water availability for irrigation and minimal necessity for harsh restriction measures until the mid-century. Under SSP585 scenario, March reservoir storage exhibits similar pattern and a slightly increased occurrence of years approaching the lower limit of the Pre-Alert threshold (2020, 2025, 2039, 2041, and 2048). Nonetheless, the WR response continues to be 25% WR, with no shift into the Alert (50% WR) or Emergency (100% WR) status throughout the simulated period. This signifies that, despite the high-emission scenario reducing water availability, simulated March reservoir storage remains above the crucial thresholds necessary for triggering stricter irrigation restrictions under current drought management policies. Notably, neither scenario yields conditions that activate Alert (50% WR) or Emergency (100% WR) status. The lack of these events indicates that the long-term average storage is limited to necessitate cautious management. This finding is consistent with the results of Lama-Pedrosa et al. (2023) for the Tormes catchment, where irrigation demands were identified as globally sustainable under current regulation conditions. Their analysis showed that the regulating capacity of reservoirs within the basin plays a key role in maintaining water availability despite fluctuations in natural runoff.

To better understand what's driving this pattern, Fig. 8 looks more closely at projected inflows under both climate scenarios. The annual inflow distributions shown in Fig. 8(a) largely overlap for SSP126 and SSP585, with a median of 432.04 and 426.68 MCM for SSP126 and SSP585 respectively. Figure 8(b) then zooms in on seasonal inflow dynamics for the year 2020, which is the last year with observed reservoir data and therefore serves as a validation reference. This single-year comparison

https://doi.org/10.5194/egusphere-2026-1502
Preprint. Discussion started: 13 April 2026

is not meant to represent long-term trends, but rather to check whether the simulations preserve the basin's characteristic seasonal recharge pattern. Both scenarios retain the strong winter and early spring inflow peaks that are crucial for replenishing the reservoir.

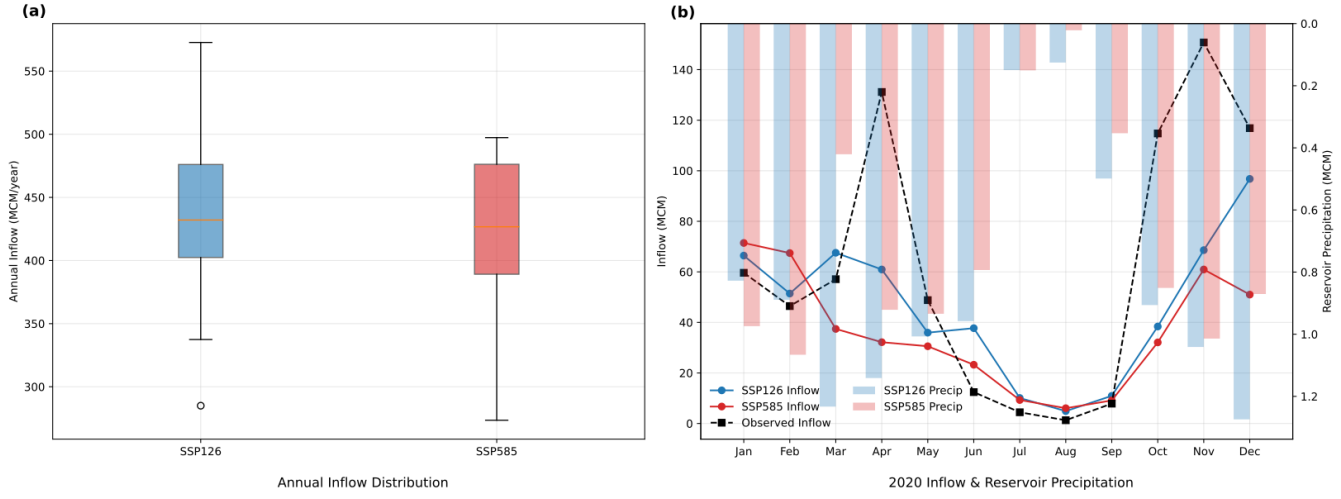

Figure 8: Projected inflow and precipitation dynamics under SSP126 and SSP585 for Santa Teresa reservoir. (a) Distribution of annual reservoir inflows for the period 2020–2050. (b) Monthly inflow and reservoir precipitation for the year 2020.

Taken together, these inflow and precipitation patterns help clarify why WR activation in Fig. 7 remains limited. Annual recharge stays relatively stable, and seasonal inflow pulses continue to refill the reservoir, keeping storage levels fluctuating near the Normal, and Pre-Alert boundary rather than pushing them toward Alert or Emergency thresholds.

This stability is further reflected in the catchment-scale water balance with (DF) and without DF (noDF) under SSP126 and SSP585 scenarios (average yearly values), which are summarized in Table 6. In general, the activation of DF results in only marginal differences across all major hydrological components. Relative changes remain below 0.5% for evapotranspiration, groundwater recharge, lateral flow, and surface runoff. In contrast, irrigation volume displays a more noticeable reduction under DF (−1.40% under SSP126 and −1.56% under SSP585), representing the largest relative change. These small variations indicate that DF primarily affects water allocation through adaptive management responses rather than altering basin-scale hydrological fluxes.

https://doi.org/10.5194/egusphere-2026-1502
Preprint. Discussion started: 13 April 2026

Table 6: Water balance components for 2020-2050 period.

Water balance component	SSP126			SSP585		
	noDF	DF	(%)	noDF	DF	(%)
Evapotranspiration (mm)	345.42	345.45	0.01	344.42	344.50	0.02
Groundwater recharge (mm)	10.02	10.01	-0.1	9.62	9.66	0.32
Lateral flow (mm)	245.22	245.20	0.0	242.41	242.59	0.07
Surface runoff (mm)	36.09	36.08	0.0	37.66	37.76	0.27
Irrigation Volume (MCM)	111.45	109.89	-1.40	117.82	115.98	-1.56

The small differences observed in water balance components at the catchment level are due to the restricted geographical extent of the farmer's crop portfolio change. Irrigated agricultural areas impacted by the WR under the drought management plan comprise around 17,596 ha (2.5%) of the overall catchment area, indicating that adaptive variations in crop portfolios, while locally relevant, do not significantly influence integrated basin water balance components. Thus, climatic forcing continues to be the main driver of basin-scale hydrology. Critically, while catchment and yearly average water balance components reveal limited responses to DF, the impacts become more pronounced at the sub-catchment and seasonal scale, especially in areas where land-use changes due to adaptive crop portfolio decisions are concentrated. This is particularly relevant since the key objective of the drought management plan and drought policy overall is to maintain streamflow throughout the year, notably during summer months where supply-demand imbalances are typically more pronounced. We look into this temporal level in the next subsection.

4.3.2 Sub-catchment-scale seasonal (summer) hydrological results

Inflow to the reservoir reflects the combined contributions of surface runoff, lateral flow, and groundwater from upstream areas, making it a useful indicator of the overall hydrological response. Figure 9 shows the percentage change in cumulative April–August inflow to the Almendra reservoir in downstream Subbasin 2, comparing simulations of DF to noDF. The years 2039 and 2048 were chosen because water restriction (WR) was activated under both SSP126 and SSP585, allowing for a consistent comparison of DF effects under similar management conditions.

https://doi.org/10.5194/egusphere-2026-1502
Preprint. Discussion started: 13 April 2026

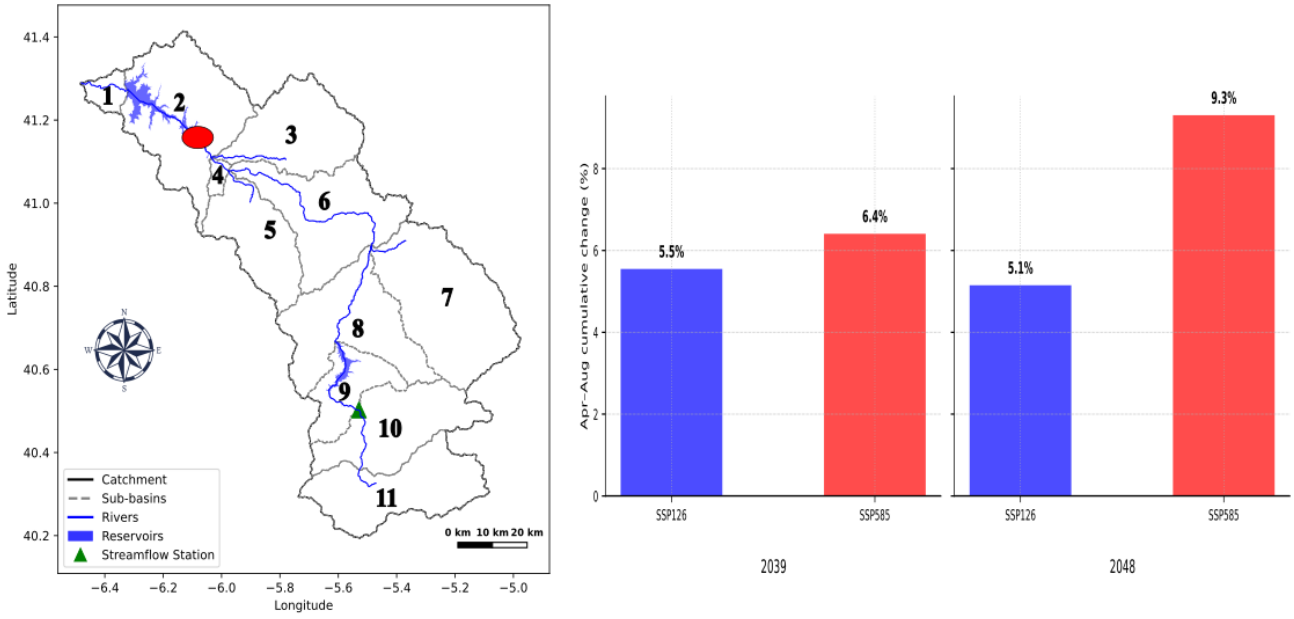

Figure 9: Relative change (%) in cumulative summer (Apr–Aug) to the Almendra reservoir in downstream Subbasin 2 for 2039 and 2048 years.

In both years and under both climate scenarios, DF leads to higher cumulative summer inflow compared to noDF. In 2039, inflow increases by 5.5% under SSP126 and 6.4% under SSP585. In 2048, the increase is 5.1% under SSP126 and rises more noticeably to 9.3% under SSP585.

Under SSP126, the effect of DF is fairly consistent across the two years, with increases of around 5.1–5.5%. Under SSP585, however, the impact is stronger, particularly in 2048. Overall, these results show that in years when WR is activated, DF is associated with higher downstream inflow to the reservoir compared to the noDF configuration, with the most pronounced response occurring under SSP585 in 2048. This is because DF significantly constrains water availability to irrigators, triggering adaptive crop portfolio changes in the irrigated area that lowers the amount of water used during the peak irrigation season and enables more of the water flow to stay in the river system (inflow to the downstream reservoir). This means that the thresholds and WR built into the drought management plan are effective in mitigating summer streamflow changes.

4.3.3 Socioeconomic impacts

Figure 10 presents the economic simulation results across different WR, including water saving and Gross Value Added (GVA, which aggregates capital income or profit and labor income). The PMAUP calibration year (2015) socioeconomic data (prices, costs) are used to calculate AWDUs reference GVA values, with GVA changes over the simulation period being measured against this reference year. GVA is measured in real prices (no changes in relative prices among crops), meaning that any changes in the adaptive response in the crop portfolio and irrigation water that impact GVA are entirely due to changes in

https://doi.org/10.5194/egusphere-2026-1502
Preprint. Discussion started: 13 April 2026

water availability under climate change and the resulting WR considered in the drought management plan. In other words, there are only four possible adaptive responses/crop portfolios and related GVA and water saving values: those under 0%, 25%, 50% and 100% WR (see Table 1). This is done to illustrate and focus on the DF coupling—alternative setups exploring different price and cost scenarios, including thorough sensitivity analysis, are feasible within SWAT-DF.

When water availability diminishes by 25%, there is a substitution of irrigated cereals by rainfed crops (mainly rainfed cereals), which leads to a marginal reduction in the GVA due to the negligible gap between irrigated and rainfed cereals' returns in the Tormes catchment (supplementary irrigation with low added value), and more significant water savings (see Fig.10 (a)). Higher GVA losses could appear under Alert, and particularly under Emergency drought where nonlinear drops in GVA of -76% are observed due to farmers being constrained to reduce the area of high-value added crops such as vegetables (blue shaded area). However, since WR never exceeded the table level (25%) in the climate change simulations, cumulative GVA reductions over 2020–2050 remain limited, amounting to approximately €1.5 million under SSP126 and €2.6 million under SSP585 relative to the noDF simulations.

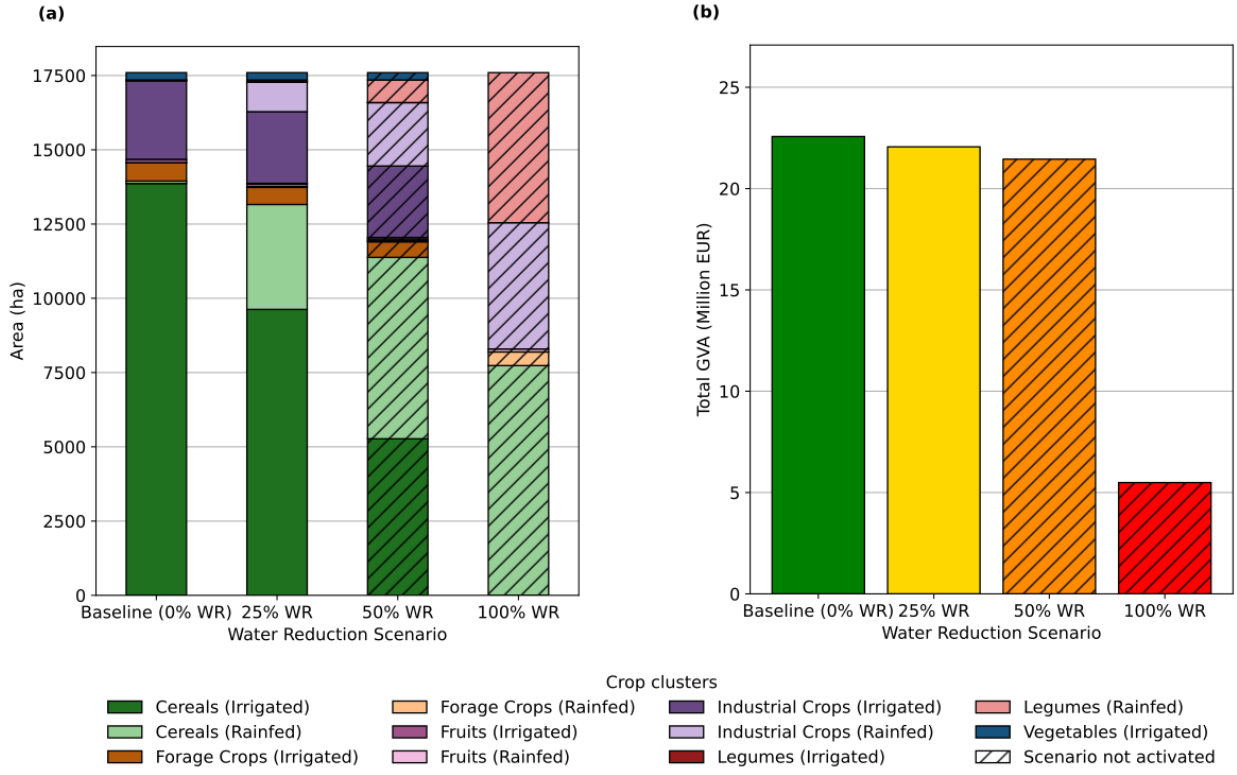

Figure 10: Impacts of WR on (a) crop portfolio, and (b) GVA, aggregated for all AWDUs. Hashed areas for the Alert and Emergency simulation results indicate these droughts thresholds never realized over 2020-2050 under hydrological and climate change scenarios considered.

https://doi.org/10.5194/egusphere-2026-1502
Preprint. Discussion started: 13 April 2026

4.4 Discussion

The methodological innovation of dynamically coupling human and water systems, as compared to conventional static or scenario-based couplings, enables a more realistic exploration of human-water systems co-evolution and interconnected responses. This study highlights several key advantages of the dynamic feedback (DF) socio-hydrological approach compared with conventional static frameworks. A major strength of endogenous coupling is that it can capture emergent behavior arising from the co-evolution of human and water systems (Di Baldassarre et al., 2019). In our simulations under SSP585, for example, the aggregated basin-scale water balance changes by less than 0.5%. In a static modeling framework, that might easily be interpreted as evidence of overall catchment resilience. The DF results, however, suggest a more differentiated interpretation. That apparent stability is maintained through strong, highly localized human adaptation. Farmers respond by replacing water-intensive irrigated cereals with rainfed alternatives, which helps preserve Gross Value Added (GVA) while also increasing critical downstream summer reservoir inflows by up to 9.3%.

We envision different research avenues to enhance the robustness and realism of the coupled DF socio-hydrological framework presented in this paper. First, the microeconomic module is calibrated in 2015, with those year's prices and costs being used to simulate the impacts of WR over the 2020-2050 period. While using a single type of scenario (climate change) allows us to place the focus on the coupling methodological design, considering alternative socioeconomic scenarios such as price changes can generate more realistic behavioral responses by agents/irrigators' with cascading impacts across human-water systems. In other words, by increasing the number and range of socioeconomic simulations in our PMAUP model, where currently only two relevant forcings related to WR are considered (as shown in Fig. 10), we would amplify the number of plausible futures and discover new market-driven co-evolution dynamics and emergent phenomena.

Second, and closely connected to the first point, crop yields were simulated based on observed data. Given the well-documented sensitivity of crop yields to climate stressors such as temperature increases, extreme weather events, and shifts in growing seasons, this likely underrepresents the full extent of climate change impacts on the agricultural production—which again calls for exploring additional scenarios (Blanc et al., 2017; Zhu et al., 2019). Third, while agricultural water demand was endogenously generated in the coupled model, water demands from industrial, urban and other uses were assumed to remain constant over time. While realistic for the depopulated and mostly agricultural Tormes catchment, this is a significant simplification that should be addressed in other catchments where our model can be tested, where future water demands may increase due to both population growth and economic development, creating increasing pressures over scarce water resources (Heidari et al., 2021; Roy et al., 2012).

Fourth, the integration of crop portfolio changes was performed at the HRU level for each AWDU under the assumption that the cultivated area of each AWDU is entirely contained within a single subbasin. When an AWDU spans multiple subbasins, reallocating crop fractions across HRUs becomes ambiguous, as the current framework cannot uniquely distribute portfolio changes while preserving subbasin-level water balance. To address this, future work should implement an automated land use mapping template that links HRUs with AWDU-level crop portfolios through a geo-spatial grid. Finally, while the coupling

https://doi.org/10.5194/egusphere-2026-1502
Preprint. Discussion started: 13 April 2026

framework can be generalized to integrate any MPM, the water system module is less flexible and can only accommodate the SWAT model (arguably one of the most widely used hydrological models). Future efforts should be made to expand the range of hydrological models that can populate the water system model and run DF simulations, possibly starting with the latest version of SWAT i.e. SWAT+.

5 Conclusion

This study presents a dynamic feedback (DF) socio-hydrological framework that explicitly captures the ongoing co-evolution of human and water systems under climate change by coupling full-fledge hydrological (SWAT) and microeconomic models (PMAUP). Methods are illustrated with an application to the Tormes catchment under CMIP6 climate scenarios (SSP126 and SSP585), where the DF setup is compared to a conventional no-feedback setup. Results show that conventional no-feedback approaches overlook important interactions between hydrological stress and adaptive human responses. A key finding is the scale dependence of these dynamics: while at the basin and annual scale differences in the overall hydrological balance between DF and no-feedback setup are small (differences remain below 0.5%), this masks stronger responses at seasonal and sub-basin scales. Under drought-triggered water restrictions, farmers adapt by shifting from more water-intensive irrigated cereals to rainfed alternatives, and this endogenous response acts as both a hydrological and economic buffer, helping maintain Gross Value Added (GVA) while increasing downstream summer inflows by up to 9.3% under SSP585 as compared to the no-feedback setup, signaling higher effectiveness of DMP interventions.

https://doi.org/10.5194/egusphere-2026-1502
Preprint. Discussion started: 13 April 2026

6 Appendices

Appendix A: Climate change scenarios

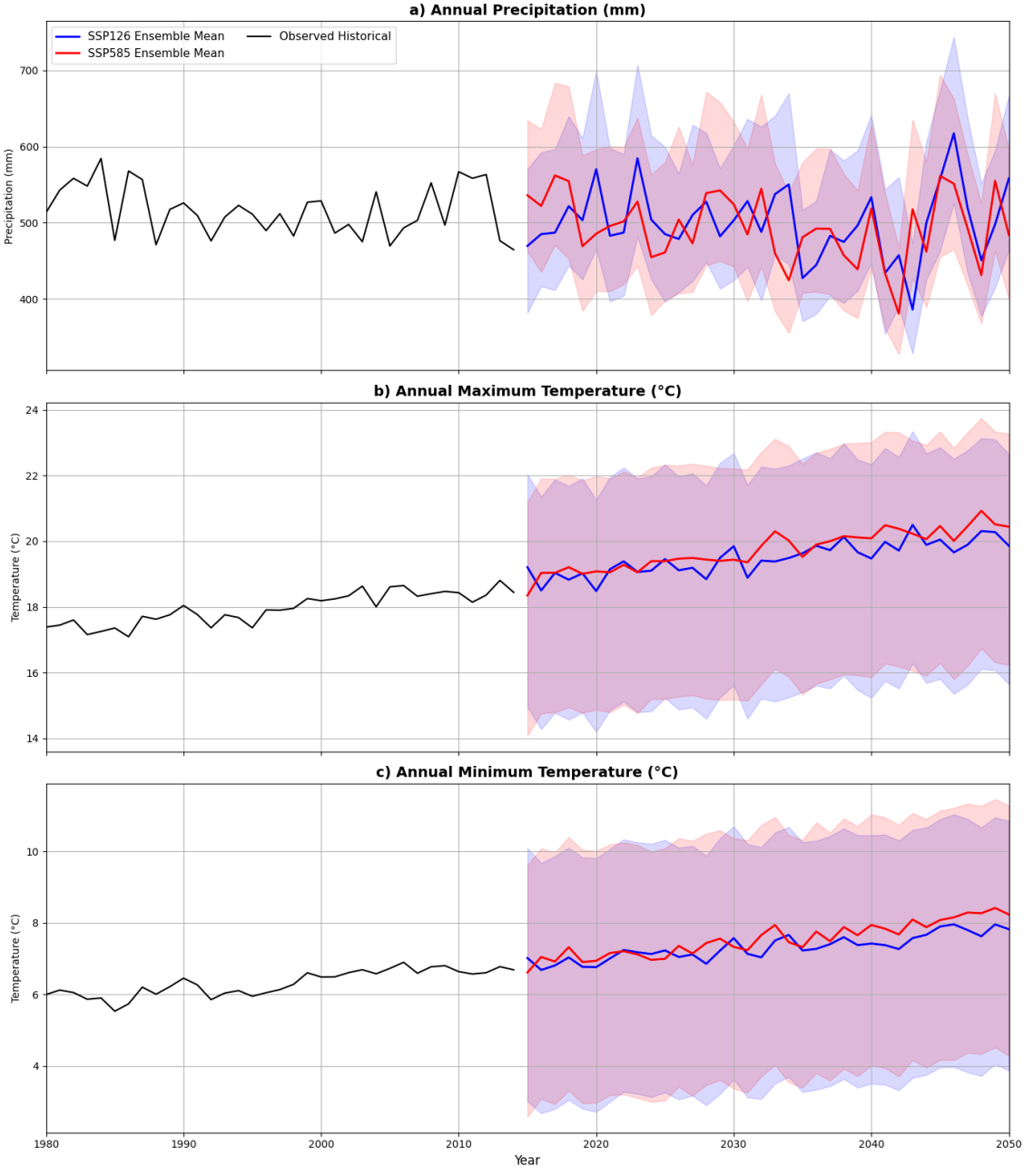

Figure A1: Multi-model ensemble projections of annual precipitation, maximum temperature, and minimum temperature for the historical (1980–2014) and future (2015–2050) periods under SSP126 and SSP585. Lines denote ensemble means and shaded areas indicate the inter-model range; historical estimates are shown in black.

https://doi.org/10.5194/egusphere-2026-1502
Preprint. Discussion started: 13 April 2026

Appendix B: Sensitivity and calibration of the SWAT model

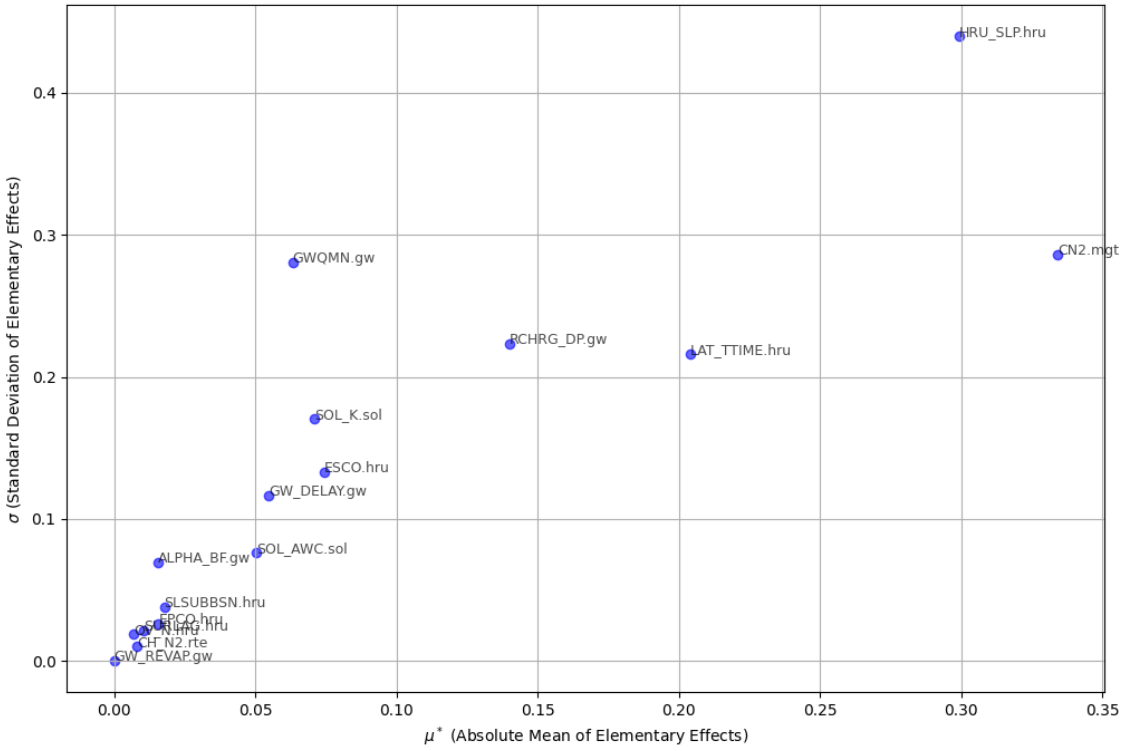

Figure B1: Morris global sensitivity analysis of model parameters (1998–2014). The mean absolute elementary effect (μ*) indicates parameter importance, while the standard deviation (σ) reflects interaction effects.

Table B1: SWAT model calibration parameters ranges and optimized values.

Parameter	Parameter description	Min	Max	Optimized
r_CN2.mgt	SCS curve number	35	98	85.85
r_ESCO.hru	Soil evaporation compensation factor	0	0.99	0.88
recohere	Plant uptake compensation factor	0	0.99	0.90
r_LAT_TTIME.hru	Lateral flow travel time (days)	0	180	13.60
r_GW_DELAY.gw	Groundwater delay time (days)	0	500	406.59
r_ALPHA_BF.gw	Baseflow alpha factor (1/days)	0	0.99	0.90
r_GWQMN.gw	Threshold water depth in the shallow aquifer for return flow (mm)	0	5000	4226.04
r_RCHRG_DP.gw	Deep aquifer percolation fraction	0	0.99	0.17
r_SOL_AWC.sol	Available water capacity of soil layer	0	1	0.12
r_SOL_K.sol	Saturated hydraulic conductivity of soil layer (mm/hr)	0	2000	1090.74
r_HRU_SLP.hru	Average slope of the HRU	0	1	0.44

https://doi.org/10.5194/egusphere-2026-1502
Preprint. Discussion started: 13 April 2026

Code and data availability

The SWAT-DF implementation is openly available on https://github.com/oshs/SWAT-DF. The PMAUP input database is available via Zenodo (https://doi.org/10.5281/zenodo.18543335). All additional data are available upon request.

Author contributions

OH: Conceptualization, Methodology, Software, Validation, Formal analysis, Data Curation, Writing – original draft, Writing – review & editing, Visualization. **FS:** Software, Data Curation, Writing – review & editing. **HG:** Software, Data Curation, Writing – review & editing. **CP:** Conceptualization, Methodology, Writing – original draft, Writing – review & editing, Supervision, Funding acquisition.

Competing interests

The authors declare that they have no conflict of interest.

Acknowledgement

This research was supported by the PIPF-2024/ECO-35944 fellowship awarded by the Comunidad de Madrid (Spain), as well as by the TRANSCEND project (Grant Agreement No. 101084110) and the European Research Council (ERC) Consolidator Grant “Water Theft” (Grant Agreement No. 101124884).

https://doi.org/10.5194/egusphere-2026-1502
Preprint. Discussion started: 13 April 2026

References

Arnold, J. G., Srinivasan, R., Muttiah, R. S., and Williams, J. R.: Large area hydrologic modeling and assessment part I: Model development, J. Am. Water Resour. Assoc., 34, 73–89, https://doi.org/10.1111/j.1752-1688.1998.tb05961.x, 1998.

Di Baldassarre, G., Viglione, A., Carr, G., Kuil, L., Salinas, J. L., and Blöschl, G.: Socio-hydrology: Conceptualising human-flood interactions, Hydrol. Earth Syst. Sci., 17, 3295–3303, https://doi.org/10.5194/hess-17-3295-2013, 2013.

Di Baldassarre, G., Sivapalan, M., Rusca, M., Cudennec, C., Garcia, M., Kreibich, H., Konar, M., Mondino, E., Mård, J., Pande, S., Sanderson, M. R., Tian, F., Viglione, A., Wei, J., Wei, Y., Yu, D. J., Srinivasan, V., and Blöschl, G.: Sociohydrology: Scientific Challenges in Addressing the Sustainable Development Goals, Water Resour. Res., 55, 6327–6355, https://doi.org/10.1029/2018WR023901, 2019.

Blair, P. and Buytaert, W.: Modelling socio-hydrological systems: a review of concepts, approaches and applications, Hydrol. Earth Syst. Sci. Discuss., 12, 8761–8851, https://doi.org/10.5194/hessd-12-8761-2015, 2015.

Blanc, E., Caron, J., Fant, C., and Monier, E.: Is current irrigation sustainable in the United States? An integrated assessment of climate change impact on water resources and irrigated crop yields, Earths Future, 5, 877–892, https://doi.org/10.1002/2016EF000473, 2017.

Bouzidi, N. and Pérez-Blanco, C. D.: A dynamic hydro-economic model to assess the effectiveness and economic benefits and costs of wetland restoration and creation, Ecosyst. Serv., 73, 101737, https://doi.org/10.1016/j.ecoser.2025.101737, 2025.

CEDEX: Centro de Estudios y Experimentación de Obras Públicas, 2023.

Choi, W. and Deal, B. M.: Assessing hydrological impact of potential land use change through hydrological and land use change modeling for the Kishwaukee River basin (USA), J. Environ. Manage., 88, 1119–1130, https://doi.org/10.1016/j.jenvman.2007.06.001, 2008.

DRBA: PLAN ESPECIAL DE SEQUÍA Demarcación Hidrográfica del Duero (Report), 2018.

ESD: The European Soil Database distribution version 2.0, European Commission and the European Soil Bureau Network, CD-ROM, EUR 19945 EN, 2004, https://doi.org/10.2905/jrc.amwqa0r, 2004.

Essenfelder, A. H., Pérez-Blanco, C. D., and Mayer, A. S.: Rationalizing Systems Analysis for the Evaluation of Adaptation Strategies in Complex Human-Water Systems, Earths Future, 6, 1181–1206, https://doi.org/10.1029/2018EF000826, 2018.

Expósito, A., Beier, F., and Berbel, J.: Hydro-Economic Modelling for Water-Policy Assessment Under Climate Change at a River Basin Scale: A Review, Water (Basel)., 12, 1559, https://doi.org/10.3390/W12061559, 2020.

Fischer, A., Miller, J. A., Nottingham, E., Wiederstein, T., Krueger, L. J., Perez-Quesada, G., Hutchinson, S. L., and Sanderson, M. R.: A Systematic Review of Spatial-Temporal Scale Issues in Sociohydrology, Frontiers in Water, 3, 730169, https://doi.org/10.3389/frwa.2021.730169, 2021.

Franzke, C. L. E., Ciullo, A., Gilmore, E. A., Matias, D. M., Nagabhatla, N., Orlov, A., Paterson, S. K., Scheffran, J., and Sillmann, J.: Perspectives on tipping points in integrated models of the natural and human Earth system: cascading effects and telecoupling, Environmental Research Letters, 17, 015004, https://doi.org/10.1088/1748-9326/ac42fd, 2022.

https://doi.org/10.5194/egusphere-2026-1502
Preprint. Discussion started: 13 April 2026

Fuka, D. R., Walter, M. T., Macalister, C., Degaetano, A. T., Steenhuis, T. S., and Easton, Z. M.: Using the Climate Forecast System Reanalysis as weather input data for watershed models, Hydrol. Process., 28, 5613–5623, https://doi.org/10.1002/hyp.10073, 2014.

Gandolfi, C., Sali, G., Facchi, A., Tediosi, A., Bulgheroni, C., Rienzner, M., and Weber, E.: Integrated modelling for agricultural policies and water resources planning coordination, Biosyst. Eng., 128, 100–112, https://doi.org/10.1016/j.biosystemseng.2014.06.006, 2014.

Gassman, P. W., Sadeghi, A. M., and Srinivasan, R.: Applications of the SWAT Model Special Section: Overview and Insights, J. Environ. Qual., 43, 1–8, https://doi.org/10.2134/jeq2013.11.0466, 2014.

Getachew, B., Manjunatha, B. R., and Bhat, H. G.: Modeling projected impacts of climate and land use/land cover changes on hydrological responses in the Lake Tana Basin, upper Blue Nile River Basin, Ethiopia, J. Hydrol. (Amst)., 595, 125974, https://doi.org/10.1016/j.jhydrol.2021.125974, 2021.

Gómez-Limón, J. A., Gutiérrez-Martín, C., and Riesgo, L.: Modeling at farm level: Positive Multi-Attribute Utility Programming, Omega (Westport)., 65, 17–27, https://doi.org/10.1016/j.omega.2015.12.004, 2016.

Gutierrez-Martin, C. and Gomez, C. M. G.: Evaluación de la mejora de la eficiencia del regadío utilizando un modelo de revelación de preferencias, Spanish Journal of Agricultural Research, 9, 1009–1020, https://doi.org/10.5424/sjar/20110904-514-10, 2011.

Haider, S., Masood, M. U., Rashid, M., Alshehri, F., Pande, C. B., Katipoğlu, O. M., and Costache, R.: Simulation of the Potential Impacts of Projected Climate and Land Use Change on Runoff under CMIP6 Scenarios, Water (Basel)., 15, 3421, https://doi.org/10.3390/w15193421, 2023.

Han, Z., Wei, Y., and Meng, J.: Representing human agency in social-hydrological models, a water (re-) allocation perspective, J. Hydrol. (Amst)., 662, 133944, https://doi.org/10.1016/j.jhydrol.2025.133944, 2025.

Harms, J. Z., Malard-Adam, J. J., Adamowski, J. F., Sharma, A., and Nkwasa, A.: Dynamically coupling system dynamics and SWAT+ models using Tinamït: Application of modular tools for coupled human-water system models, Hydrol. Earth Syst. Sci., 27, 1683–1693, https://doi.org/10.5194/hess-27-1683-2023, 2023.

Harou, J. J., Medellín-Azuara, J., Zhu, T., Tanaka, S. K., Lund, J. R., Stine, S., Olivares, M. A., and Jenkins, M. W.: Economic consequences of optimized water management for a prolonged, severe drought in California, Water Resour. Res., 46, https://doi.org/10.1029/2008WR007681, 2010.

Heidari, H., Arabi, M., and Warziniack, T.: Vulnerability to Water Shortage Under Current and Future Water Supply-Demand Conditions Across U.S. River Basins, Earths Future, 9, https://doi.org/10.1029/2021EF002278, 2021.

IGN: Instituto Geográfico Nacional: Cartografía y Datos geográficos., 2020.

Jeuland, M.: Economic implications of climate change for infrastructure planning in transboundary water systems: An example from the Blue Nile, Water Resour. Res., 46, 11556, https://doi.org/10.1029/2010WR009428, 2010.

Kahil, M. T., Dinar, A., and Albiac, J.: Modeling water scarcity and droughts for policy adaptation to climate change in arid and semiarid regions, J. Hydrol. (Amst)., 522, 95–109, https://doi.org/10.1016/J.JHYDROL.2014.12.042, 2015.

https://doi.org/10.5194/egusphere-2026-1502
Preprint. Discussion started: 13 April 2026

Konar, M., Garcia, M., Sanderson, M. R., Yu, D. J., and Sivapalan, M.: Expanding the Scope and Foundation of Sociohydrology as the Science of Coupled Human-Water Systems, Water Resour. Res., 55, 874–887, https://doi.org/10.1029/2018WR024088, 2019.

Lama-Pedrosa, B., Sordo-Ward, Á., Bianucci, P., and Garrote, L.: Sustainability of Duero Water Systems for Crop Production in Spain, Sustainability, 16, 242, https://doi.org/10.3390/su16010242, 2023.

Laniak, G. F., Olchin, G., Goodall, J., Voinov, A., Hill, M., Glynn, P., Whelan, G., Geller, G., Quinn, N., Blind, M., Peckham, S., Reaney, S., Gaber, N., Kennedy, R., and Hughes, A.: Integrated environmental modeling: A vision and roadmap for the future, Environmental Modelling & Software, 39, 3–23, https://doi.org/10.1016/j.envsoft.2012.09.006, 2013.

MAGRAMA: Anuario de Estadística Agraria (Agricultural Statistics Yearbook) (Report). Ministerio de Agricultura, Alimentación y Medio Ambiente, Madrid, 2015a.

MAGRAMA: Estudios de costes y rentas de las explotaciones agrarias (Database). Ministerio de Agricultura, Alimentación y Medio Ambiente, Madrid, 2015b.

Moriasi, D. N., Arnold, J. G., Liew, M. W. Van, Bingner, R. L., Harmel, R. D., and Veith, T. L.: Model evaluation guidelines for systematic quantification of accuracy in watershed simulations, Trans. ASABE, 50, 885–900, https://doi.org/10.13031/2013.23153, 2007.

Morris, M. D.: Factorial Sampling Plans for Preliminary Computational Experiments, Technometrics, 33, 161, https://doi.org/10.2307/1269043, 1991.

Nguyen, T. V., Dietrich, J., Dang, T. D., Tran, D. A., Van Doan, B., Sarrazin, F. J., Abbaspour, K., and Srinivasan, R.: An interactive graphical interface tool for parameter calibration, sensitivity analysis, uncertainty analysis, and visualization for the Soil and Water Assessment Tool, Environmental Modelling & Software, 156, 105497, https://doi.org/10.1016/j.envsoft.2022.105497, 2022.

Nie, W., Yuan, Y., Kepner, W., Nash, M. S., Jackson, M., and Erickson, C.: Assessing impacts of Landuse and Landcover changes on hydrology for the upper San Pedro watershed, J. Hydrol. (Amst)., 407, 105–114, https://doi.org/10.1016/j.jhydrol.2011.07.012, 2011.

Reshma, C. and Arunkumar, R.: Assessment of impact of climate change on the streamflow of Idamalayar River Basin, Kerala, Journal of Water and Climate Change, 14, 2133–2149, https://doi.org/10.2166/wcc.2023.456, 2023.

Roobavannan, M., Kandasamy, J., Pande, S., Vigneswaran, S., and Sivapalan, M.: Sustainability of agricultural basin development under uncertain future climate and economic conditions: A socio-hydrological analysis, Ecological Economics, 174, 106665, https://doi.org/10.1016/j.ecolecon.2020.106665, 2020.

Roy, S. B., Chen, L., Girvetz, E. H., Maurer, E. P., Mills, W. B., and Grieb, T. M.: Projecting water withdrawal and supply for future decades in the U.S. under climate change scenarios, Environ. Sci. Technol., 46, 2545–2556, https://doi.org/10.1021/ES2030774, 2012.

https://doi.org/10.5194/egusphere-2026-1502
Preprint. Discussion started: 13 April 2026

Samimi, M., Mirchi, A., Moriasi, D., Ahn, S., Alian, S., Taghvaeian, S., and Sheng, Z.: Modeling arid/semi-arid irrigated agricultural watersheds with SWAT: Applications, challenges, and solution strategies, J. Hydrol. (Amst)., 590, 125418, https://doi.org/10.1016/j.jhydrol.2020.125418, 2020.

Sapino, F., Pérez-Blanco, C. D., Gutiérrez-Martín, C., and Frontuto, V.: An ensemble experiment of mathematical programming models to assess socio-economic effects of agricultural water pricing reform in the Piedmont Region, Italy, J. Environ. Manage., 267, 110645, https://doi.org/10.1016/j.jenvman.2020.110645, 2020.

Senent-Aparicio, J., Jimeno-Sáez, P., López-Ballesteros, A., Giménez, J. G., Pérez-Sánchez, J., Cecilia, J. M., and Srinivasan, R.: Impacts of swat weather generator statistics from high-resolution datasets on monthly streamflow simulation over Peninsular Spain, J. Hydrol. Reg. Stud., 35, 100826, https://doi.org/10.1016/J.EJRH.2021.100826, 2021.

Soriano, G., Sapino, F., and Pérez-Blanco, C. D.: A review of economic calibrated mathematical programming models for agricultural water reallocation, Environmental Modelling & Software, 106628, https://doi.org/10.1016/j.envsoft.2025.106628, 2025.

Souza da Silva, G. N. and de Moraes, M. M. G. A.: Economic water management decisions: trade-offs between conflicting objectives in the sub-middle region of the São Francisco watershed, Reg. Environ. Change, 18, 1957–1967, https://doi.org/10.1007/S10113-018-1319-5, 2018.

Thrasher, B., Wang, W., Michaelis, A., Melton, F., Lee, T., and Nemani, R.: NASA Global Daily Downscaled Projections, CMIP6, Sci. Data, 9, 262, https://doi.org/10.1038/s41597-022-01393-4, 2022.

Vanelli, F. M., Kobiyama, M., and de Brito, M. M.: To which extent are socio-hydrology studies truly integrative? The case of natural hazards and disaster research, Hydrol. Earth Syst. Sci., 26, 2301–2317, https://doi.org/10.5194/hess-26-2301-2022, 2022.

Voinov, A. and Shugart, H. H.: 'Integronsters', integral and integrated modeling, Environmental Modelling & Software, 39, 149–158, https://doi.org/10.1016/j.envsoft.2012.05.014, 2013.

Yen, H., Park, S., Arnold, J. G., Srinivasan, R., Chawanda, C. J., Wang, R., Feng, Q., Wu, J., Miao, C., Bieger, K., Daggupati, P., van Griensven, A., Kalin, L., Lee, S., Sheshukov, A. Y., White, M. J., Yuan, Y., Yeo, I. Y., Zhang, M., and Zhang, X.: IPEAT+: A built-in optimization and automatic calibration tool of SWAT+, Water (Basel)., 11, https://doi.org/10.3390/w11081681, 2019.

Zhang, X. and He, Y.: Impact of Climate Change and Human Activities to Runoff in the Du River Basin of the Qinling-Daba Mountains, China, Remote Sens. (Basel)., 15, https://doi.org/10.3390/rs15215178, 2023.

Zhu, X., Troy, T. J., and Devineni, N.: Stochastically modeling the projected impacts of climate change on rainfed and irrigated US crop yields, Environmental Research Letters, 14, https://doi.org/10.1088/1748-9326/AB25A1, 2019.